Liquid Crystals
Publication details, including instructions for authors and subscription information:
http://www.informaworld.com/smpp/title~content=t713926090

In situ determination of glass transition temperatures in thin polymer films

C. Benecke[a]; K. Schmitt[a]; M. Schadt[a]
[a] ROLIC Ltd, Basel, Switzerland

To cite this Article Benecke, C. , Schmitt, K. and Schadt, M.(1996) '*In situ* determination of glass transition temperatures in thin polymer films', Liquid Crystals, 21: 4, 575 — 580
To link to this Article: DOI: 10.1080/02678299608032865
URL: http://dx.doi.org/10.1080/02678299608032865

LIQUID CRYSTALS, 1996, VOL. 21, NO. 4, 575–580

In situ determination of glass transition temperatures in thin polymer films

by C. BENECKE*, K. SCHMITT, and M. SCHADT
ROLIC Ltd, Grenzacherstr. 124, CH-4002 Basel, Switzerland

(*Received 5 February 1996; accepted 5 May 1996*)

A method for determining the glass transition temperature T_g of waveguiding NLO-films is presented. This enables for the first time monitoring of the T_g of NLO-films on device substrates *in situ*. T_g is shown to follow from the temperature dependencies of the refractive index $n(T)$ or the thickness $d_f(T)$ of thin films.

1. Introduction

The glass transition temperature T_g is a fundamental parameter of the macroscopic and microscopic properties of non-crystalline polymers [1–3]. Therefore, T_g belongs to the standard analytical parameters to be evaluated for characterizing a polymeric material. Particularly in the case of poled NLO-polymers for second order NLO-applications, T_g is an important parameter for predicting the thermal stability [4] of the field-induced non-centrosymmetric configuration of the polymer matrix and for adjusting the poling temperature during sample preparation. Furthermore, in cross-linkable polymers, T_g strongly depends on the cross-linking density and is therefore a measure for the degree of cross-linking of the material.

T_g is usually measured by differential scanning calorimetry (DSC), requiring typically a few milligrams of powdered material. This method is well established and has been proven to be reliable if carefully performed. However, in particular cases where the material under consideration is not accessible as a meltable powder, or when it is part of a complex sample, the DSC technique is no longer applicable. Such a situation is often encountered in polymer waveguide experiments where the film is intimately connected to a substrate and where the solid state configuration of the layer material differs from that of the original polymer powder. Photo-cross-linkable NLO-polymers are an illustrative example. In this case, the polymer film is prepared from uncross-linked material on glass substrates and is then simultaneously poled and cross-linked. Both treatments induce changes of T_g. To determine the T_g of polymeric thin films which are part of NLO-devices, we have developed a method which is applicable *in situ* during waveguide preparation.

2. Experimental

The waveguides used in our investigations were designed such that (1) selective and efficient mode excitation results and (2) the polymer film surfaces were freely accessible. This was accomplished by a modified prism coupling scheme shown in figure 1 (*a*), where the substrate consists of a high index glass prism covered with a 4 µm thick sputtered quartz layer in the central part of the prism base. The polymer layer was placed on top of this structure covering the entire prism area. The laser beam was incident from the prism side, entering the waveguide at the edge of the quartz layer. In our design, the low index 's'-shaped edge plays the role of the air gap of conventional prism coupling schemes. As Ulrich [5] has theoretically shown, the coupling efficiency strongly depends on the profile of the quartz edge. Therefore, we approximated the ideal shape by sputtering the quartz material through a shadow mask, see figure 1 (*b*) [5, 6]. For poling purposes, a thin ITO layer was sputtered on top of the quartz layer. This ITO layer was laterally structured by standard techniques. The NLO-polymer films were prepared by spin coating. For our experiments we used two different polymers synthesized in our laboratories, namely: **P1** (T_g(DSC)$\approx$75°C; 20 K min^{-1}) and **P2** (T_g(DSC)$\approx$81°C; 20 K min^{-1}). The structures of these polymers consist of a cross-linkable side chain comprising an azo chromophore attached to the backbone:

For structural details of the polymers see reference [7].

3. Results and discussion

Mode spectra of TE and TM modes excited with s and p polarised HeNe laser light were analyzed using the standard procedure described by Ulrich [5]. In the simplest case of a three layer structure consisting of homogeneous and isotropic materials, the coupling angles of two guided modes have previously been shown to be required in order to determine film thickness and

---

*Author for correspondence.

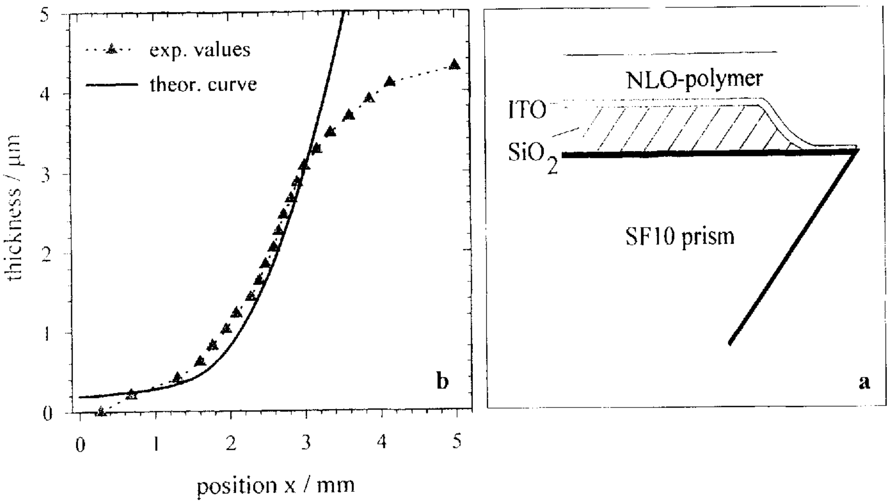

Figure 1. (*a*) Prism coupling scheme. (*b*) Comparison between the experimental and theoretical coupling edge shape. Parameters for the theoretical curve: $\lambda = 632\,\mathrm{nm}$; $n_c = 1{\cdot}0$; $n_f = 1{\cdot}64$; $n_{\mathrm{prism}} = 1{\cdot}723$. (SF10); $d_f = 1{\cdot}0\,\mu\mathrm{m}$; mode = TE; beamwidth = $400\,\mu\mathrm{m}$.

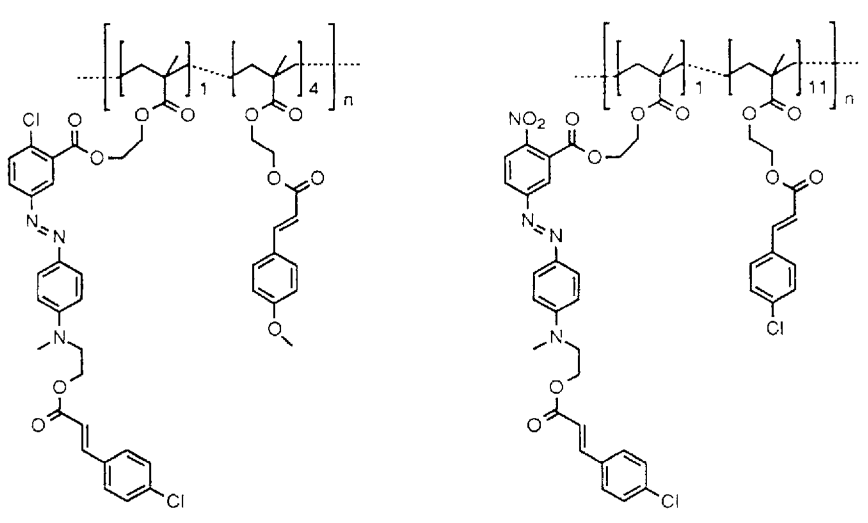

P1 **P2**

Structural formulae of polymers **P1** and **P2**

refractive index [8]. In sufficiently thick films, more than two modes can be excited. This allows the validity of the model to be checked and evaluation of the increased number of parameters characterizing complex geometries. For example, an anisotropic three layer structure or an isotropic four layer structure require three and four parameters, respectively [9, 10].

For both the three layer and the four layer cases, we verified the validity of the respective models. If the deviations δd_f and δn_f of the theoretical and the experimental coupling angles were below a certain limit the model was accepted. As an example, figure 2 shows a series of mode spectra (*a*), (*c*), (*d*), (*f*) belonging to polymer layers which we exposed during different times, t_{exp}. In the central part (*b*) & (*e*) of figure 2, the dispersions of two characteristic cases are plotted. The upper graph (*b*) reflects the isotropic case, whereas the lower graph (*e*) corresponds to an uniaxial NLO-film. The two graphs (*a*) & (*d*) on the left show the respective mode spectra. Interestingly the TM and TE modes cross in the anisotropic case.

From the mode spectra and the Sellmeier equation [11]:

$$n(\lambda) = \left(\frac{q}{\lambda_0^{-2} - \lambda^{-2}} + A\right)^{1/2}$$

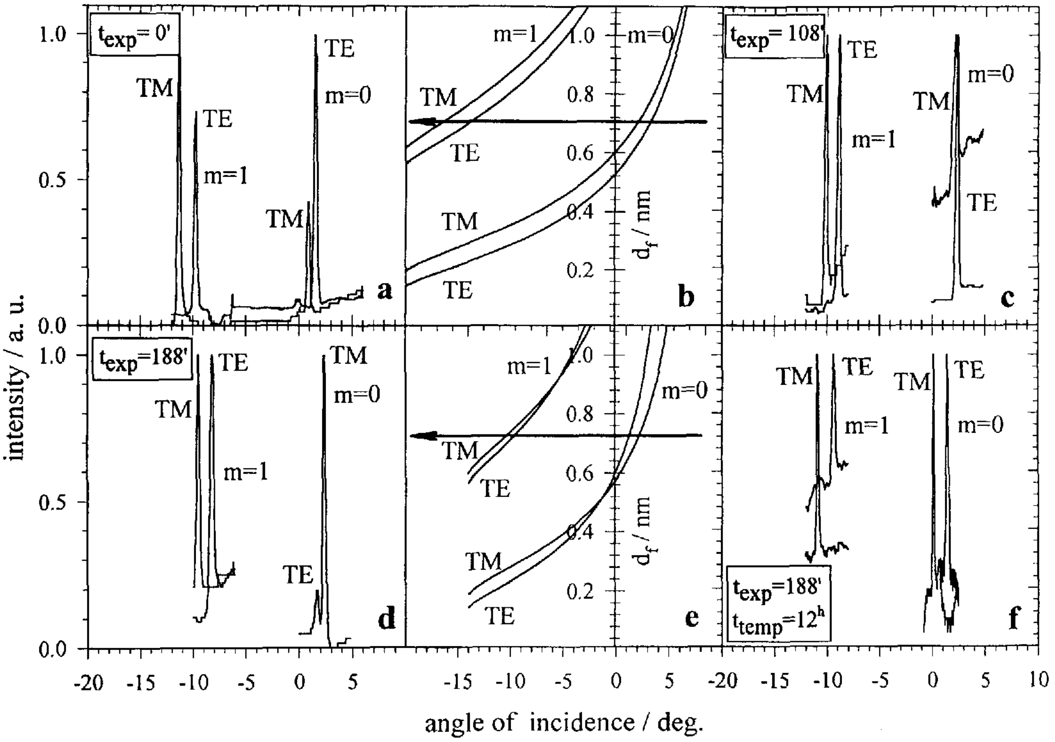

Figure 2. Mode spectra as a function of exposure time, t_{exp}, and the related dispersion curves. Polymer = **P1**, temperature = RT, $\lambda = 632\,\mathrm{nm}$, $d_f = 720\,\mathrm{nm}$; Philips UV-lamp 250W, and filter UG11/3 mm, (0·4–0·8) mW cm^{-2}.

the refractive indices $n(\lambda)$ were extracted and are summarised in the table. The three parameters (q, λ_0, A) in the table were treated as free fit variables. The last column of the table shows the experimental values of the absorption maxima, λ_{abs}. The λ_{abs} values are in reasonable agreement with the respective Sellmeier constants λ_0.

Figure 3 shows that the refractive indices of our NLO-polymers differ by $\approx$0·035. This small deviation is due mainly to the different chromophore concentration and the different position of the absorption band. The batch to batch fluctuations are negligible. The Sellmeier curves of the respective pair of non-cross-linked and cross-linked polymers are plotted in figure 3.

The influence of cross-linking on the refractive index of NLO-polymers following from figure 3 is striking. This is a consequence of the 2+2 cyclo-addition which destroys the conjugation of the cinnamic ester moiety leading to a decrease of *n*.

Table. Sellmeier coefficients (q, λ_o, A) of the NLO-polymers and the wavelength of the absorption band λ_{abs}; (CL = cross-linked).

NLO-polymer	λ_o/nm	A	$q/10^{-6}\,\mathrm{nm}^{-2}$	λ_{abs}/nm
P2 non-CL	458·75	2·3635	0·466	460
P2 CL	410·0	2·293	1·00	460
P1 non-CL	411·11	2·3406	1·24	425
P1 CL	418·7	2·345	1·00	425

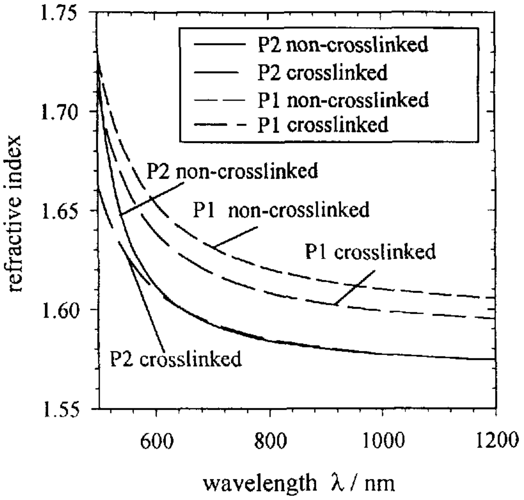

Figure 3. Dispersion curves of two (non)-cross-linked NLO-polymers.

Cross-linking is accompanied by photo-bleaching of the cinnamic acid absorption band at about 310 nm. The dynamics of this process have been investigated in detail by Moshrefzadeh *et al.* [12(*a*)] and Diemeer *et al.* [12(*b*)] for a chromophore doped polymer. Due to the high absorption coefficient of the chromophore, light incident on the sample from one side is completely absorbed within a thin layer of unbleached material. This leads to splitting of the waveguiding layer into a bleached and cross-linked upper part, and an unbleached lower part with a sharp interface between the sublayers. With extended exposure, this interface travels through the layer and at last reaches the substrate. Therefore, the NLO-layer is isotropic and homogeneous at the beginning and can be described by a three layer model. At an intermediate cross-linking stage the layer is inhomogeneous and consists of two sublayers; it must then be described by a four layer model. At the end of the cross-linking process, the NLO-layer is once more homogeneous and therefore compatible again with a three layer model.

Since for device preparation a simple and generally applicable determination of the minimal exposure time for complete cross-linking is required, the following procedure was developed. Assuming constant layer thickness, we used the three layer model analysis as an indicator for determining the state of progress of the cross-linking. At $t_{\mathrm{exp}}=0$, the index of refraction n and the layer thickness d_{f} of the uncross-linked polymer were determined. At intermediate stages of exposure, the layer becomes inhomogeneous, and hence the three layer model leads to differing values for n, namely n^{TE} and n^{TM}. n^{TE} and n^{TM} depend on the mode (i.e. TE_0 or TM_0, respectively) used for determining n. For $t_{\mathrm{exp}}>120\,\mathrm{min}$, these indices converge to a common isotropic value. This is shown in figure 4. Convergence also proves the validity of the assumed constancy of the overall layer thickness.

Next we studied whether determining T_{g} by waveguiding can be used as a non-destructive *in-situ* method for cross-linked polymeric films. Figure 5 shows the change of the refractive index at $T<T_{\mathrm{g}}$ of a bulk sample of the non-cross-linked NLO-polymer **P2** determined with an Abbé refractometer and, for comparison, values determined in a waveguide experiment. Apart from a small off-set of $|n(\mathrm{waveguiding})\text{-}n(\mathrm{Abbé})|\approx 0{\cdot}0025$, figure 5 shows that the data of the two methods agree. Our method reveals a change in the temperature gradient $\partial n/\partial T$ at a temperature which is identical with $T_{\mathrm{g}}(\mathrm{DSC})$. This proves that the phase transition can indeed be determined from the $n(T)$ graph of waveguiding experiments.

Figure 6 shows the temperature dependence of n and of d_{f} of polymer **P1**. Also in this case a distinct change of the temperature gradient of the refractive index was found at T^*. Furthermore, an increase of T^* after 2 hours of exposure at about 20°C is noticeable in the cross-linked polymer (figure 6). However, the change of the temperature gradient at T^* for the non-cross-linked polymer is 18°C below T_{g} determined by DSC measurements (figure 6). This may be due to a modified distribution of the free volume in thin films compared with the respective distribution in bulk samples. As stated by Prêtre *et al.* [13], T_{g} is a kinetic phenomenon depending on the rate of cooling; since the signal heights in DSC experiments strongly depend on the cooling or heating rates, these rates cannot be reduced too much if small differences of heat capacity are to be detected. In the case of our polymers, a rate of $20\,\mathrm{K\,min}^{-1}$ was found to be adequate. For higher cooling rates, higher T_{g} values resulted. Indeed, careful measurements of T_{g} using decreasing cooling rates lead to decreasing T_{g} values.

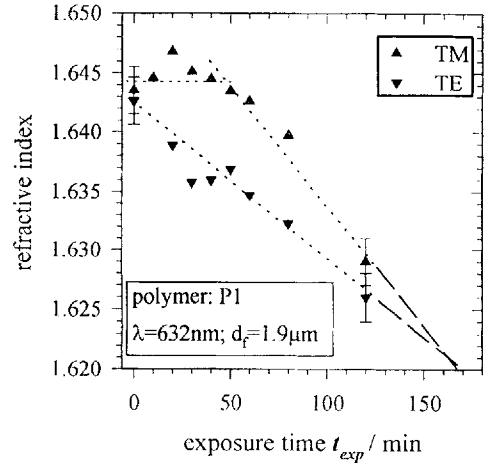

Figure 4. Refractive index n vs. exposure time t_{exp} of an NLO-polymer film (**P1**), $\lambda=623\,\mathrm{nm}$, $d_{\mathrm{f}}=1{\cdot}9\,\mu\mathrm{m}$; Philips UV-lamp 250 W, and filter UG11/3 mm, $(0{\cdot}4\text{–}0{\cdot}8)\,\mathrm{mW\,cm}^{-2}$.

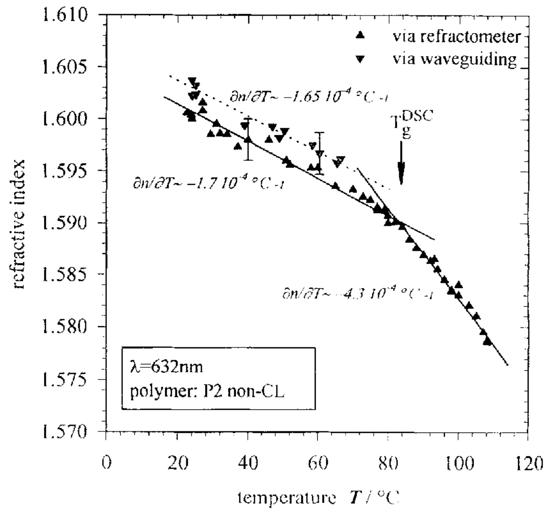

Figure 5. Refractive index n vs. temperature T; $\lambda=632\,\mathrm{nm}$, polymer = **P2** non-cross-linked. T_{g} (DSC) glass temperature determined by DSC measurement.

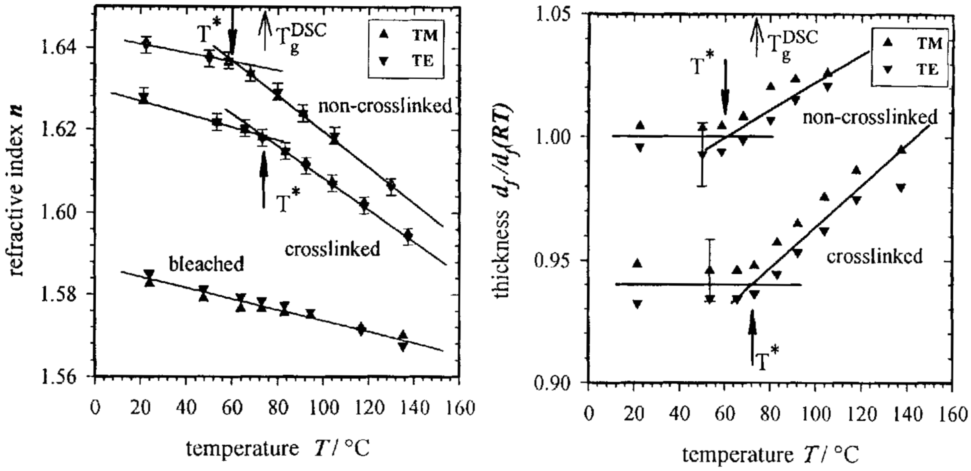

Figure 6. Refractive index and normalised film thickness vs. temperature ($\lambda = 632$ nm) for polymer **P1** non-cross-linked, cross-linked ($t_{CL} = 2^h$ with UG11/3 filter) and bleached ($t_{bleached} \approx 24^h$ complete decolourisation with 375 nm filter); Philips UV-lamp.

On the other hand, our waveguide samples were tempered at 120°C for 12 h and then slowly cooled down to room temperature within 10 h. To avoid temperature gradients within the samples, the films were allowed to equilibrate for 15 min at each temperature before recording the mode spectra. Thus, our waveguide experiments are static, whereas DSC measurements are dynamic. On the other hand, a modified distribution of the free volume may have been induced by our sample preparation technique. However, this distribution, which is suspected to be far away from thermodynamic equilibrium, is allowed to relax in the course of the tempering process. Therefore, the final distribution will probably approach that of bulk samples. The decreasing refractive index in the case of our cross-linked polymers is mainly due to the 2+2 cyclo-addition of the cinnamate groups and to a smaller degree to the degradation of the NLO-chromophores. No differences of n^{TE} and n^{TM} are noticeable, whereas small deviations in d_f^{TE} and d_f^{TM} follow from figure 6.

The difference $\Delta d_f \approx 20$ nm between d_f^{TE} and d_f^{TM}, which is within the standard deviation of d_f may be due to a small anisotropy of the film. For $T < T_g$, the thickness is almost constant, indicating a small thermal expansion coefficient. But if T exceeds T_g, the film thickness increases constantly, indicating a larger thermal expansion coefficient. In the case of fully cross-linked and bleached films, no more changes in temperature gradients occurred. From figure 6, it follows that the gradients $\partial n/\partial T$ for cross-linked and non-cross-linked films are similar for $T < T_g$.

4. Conclusion

We have shown that optical waveguide experiments can be used to determine the glass transition temperatures of thin polymer films *in situ*. Moreover, the process of cross-linking can be monitored with our technique. In particular, this new, non-destructive optical method allows analysis of the cross-linking dependence of T_g during UV-light exposure in complex waveguiding structures. Our method results in glass transition temperatures which are a few degrees below those determined in separate experiments and with separate samples by DSC. The deviation is attributed to the different physical parameters of the samples. The sensitivity of our method depends on how accurately the refractive indices of the film can be determined. Assuming an accuracy of $n \approx 0{\cdot}001$, a change of the slope $\partial n/\partial T$ of the order of 10^{-4} (°C^{-1}) is sufficient to determine the phase transition temperature with our technique. It should be added that our optical approach is not restricted to samples deposited on specific waveguiding substrates. Any coupling scheme which allows generation of mode selective coupling, such as grating couplers, etc., is equally well suited. Moreover, our method is not restricted to amorphous polymer films, but can equally well be applied to liquid crystalline polymers (LCPs) and LCP-networks. This will be shown in a subsequent publication on novel LCP-waveguides exhibiting light scattering losses below 1 dB cm^{-1}.

We gratefully acknowledge fruitful discussions with A. Schuster and S. M. Kelly. Also we thank R. Genini and J. Däscher for technical assistance.

References

[1] Bosshard, Ch., Sutter, K., Prêtre, P., Hulliger, J., Flörsheimer, M., Kaatz, P., and Günter, P., 1995, *Organic Nonlinear Optical Materials Advances*, Nonlinear Optics Vol.1 (Gordon and Breach).

[2] Prasad, P. N., and Williams, D. J., 1991, *Introduction to Nonlinear Optical Effects in Molecules and Polymers*, (Wiley & Son).

[3] Man, H.-T., and Yoon, H. N., 1992, *Adv. Mat.*, **4,** 159.

[4] Lytel, R., Lipscomb, G. F., Binkley, E. S., Kenney, J. T., and Ticknor, A. J., 1991, *ACS Symp. Ser.*, **445,** 103.

[5] Ulrich, R., 1971, *J. opt. Soc. A.*, **61,** 1467.

[6] Schmitt, K., Herr, R. P., Schadt, M., Fünfschilling, J., Buchecker, R., Chen, X. H., and Benecke, C., 1993, *Liq. Cryst.*, **14,** 1735.

[7] Schmitt, K., *et al.* (to be published).

[8] Marcuse, M., 1992, *Dielectric Waveguides*, (Pergamon Press).

[9] Burns, W. K., and Warner, J., 1974, *J. opt. Soc. A.*, **64,** 441.

[10] Adams, M. J., 1981, *An Introduction to Optical Waveguides*, (J. Wiley & Sons).

[11] Born, M., and Wolf, E., 1989, *Principles of Optics* (Pergamon Press).

[12] (*a*) Moshrefzadeh, R. S., Misemer, D. K., Radcliffe, M. D., Francis, C. V., and Mohapatra, S. K., 1993, *Appl. Phys. Lett.*, **62,** 16; (*b*) Diemeer, M. B. J., Suyten, F. M. M., Trommel, E. S., McDonach, A., Copeland, J. M., Jenneskens, L. W., and Horsthuis, W. H. G., 1990, *Electron. Lett.*, **26,** 379.

[13] Prêtre, P., Kaatz, P., Bohren, A., Günter, P., Zysset, B., Ahlheim, M., Stähelin, M., Lehr, F., 1994, *Macromol.*, **27,** 5476.